Research in Astronomy and Astrophysics, 22:045015 (9pp), 2022 April https://doi.org/10.1088/1674-4527/ac55ff

The Nonlinear Field Equation of the Three-point Correlation Function of Galaxies: to the Second Order of Density Perturbation

Shu-Guang Wu and Yang Zhang
Department of Astronomy, Key Laboratory for Researches in Galaxies and Cosmology, University of Science and Technology of China, Hefei 230026, China
wusg@mail.ustc.edu.cn, yzh@ustc.edu.cn
Received 2022 January 1; revised 2022 February 11; accepted 2022 February 15; published 2022 March 31

Abstract

Based on the field theory of density fluctuation under Newtonian gravity, we obtain analytically the nonlinear equation of 3-pt correlation function ζ of galaxies in a homogeneous, isotropic, static universe. The density fluctuation has been kept up to second order. By the Fry–Peebles ansatz and the Groth-Peebles ansatz, the equation of ζ becomes closed and differs from the Gaussian approximate equation. Using the boundary condition inferred from the data of SDSS, we obtain the solution $\zeta(r, u, \theta)$ at fixed $u = 2$, which exhibits a shallow U-shape along the angle θ and, nevertheless, decreases monotonously along the radial r. We show its difference with the Gaussian solution. As a direct criterion of non-Gaussianity, the reduced $Q(r, u, \theta)$ deviates from the Gaussianity plane $Q = 1$, exhibits a deeper U-shape along θ and varies weakly along r, agreeing with the observed data.

Key words: gravitation – hydrodynamics – cosmology: large-scale structure of universe

1. Introduction

The n-point correlation functions are important tools to study the statistical properties of matter distribution on the large scale of the universe and can provide fundamental tests of the standard cosmological model (Peebles 1980; Bernardeau et al. 2002). The statistic of noninteracting particles, like CMB, can be well described a statistically Gaussian random field, the 2-point correlation function (2PCF) will be sufficient to characterize its correlation. When long-range Newtonian gravity is taken into account, the concept of a Gaussian random field has been subtle in literature so far. Therefore, a criterion of non-Gaussianity is required to be defined clearly. The equation of 2PCF $G^{(2)}(r)$ of density fluctuation to lowest order under Newtonian gravity is a Helmholtz equation with a delta source, and the exact solution has been given and called the solution in the Gaussian approximation in Zhang (2007). This is because the equation $G^{(2)}(r)$ shares a structure similar to the Gaussian approximate equation (Goldenfeld 1992) that has been commonly used in condensed matter physics. Parallelly, the equation of 3-pt correlation function (3PCF) of density fluctuation to the lowest order (the Gaussian approximation) is also a linear equation and the exact solution (Zhang et al. 2019) has been found as the following

$$G^{(3)}(r_{12}, r_{23}, r_{31}) = Q[G^{(2)}(r_{12})G^{(2)}(r_{23}) + G^{(2)}(r_{23})G^{(2)}(r_{31}) + G^{(2)}(r_{31})G^{(2)}(r_{12})] \tag{1}$$

where $Q = 1$, and $r_{12} = |\boldsymbol{r}_1 - \boldsymbol{r}_2|$, etc. Thus, $Q = 1$ holds in the Gaussian approximation, and any deviation of Q from 1 will be an indication of non-Gaussianity of the density fluctuation. Interestingly, the solution (1) in the Gaussian approximation is exactly the content of the Groth-Peebles ansatz with $Q = 1$ (Groth & Peebles 1975, 1977). When density fluctuations up to second order are included, the equations of $G^{(2)}(r)$ becomes nonlinear (Zhang & Miao 2009; Zhang & Chen 2015; Zhang et al. 2019), and its solution describes the distribution of galaxies better than the Gaussian approximation at small scales. But $G^{(3)}$ has not been analytically studied up to second order of density fluctuation. Statistically, $G^{(3)}(\boldsymbol{r}, \boldsymbol{r}', \boldsymbol{r}'')$ describes the excess probability over random of finding three galaxies located at the three vertices $(\boldsymbol{r}, \boldsymbol{r}', \boldsymbol{r}'')$ of a given triangle. In observations and numerical studies, as an extension of the Groth-Peebles ansatz (1), the reduced 3PCF is often introduced

$$Q(\boldsymbol{r}, \boldsymbol{r}', \boldsymbol{r}'') \equiv \frac{G^{(3)}(\boldsymbol{r}, \boldsymbol{r}', \boldsymbol{r}'')}{G^{(2)}(\boldsymbol{r}, \boldsymbol{r}')G^{(2)}(\boldsymbol{r}', \mathrm{r}'') + G^{(2)}(\boldsymbol{r}', \mathrm{r}'')G^{(2)}(\boldsymbol{r}'', \boldsymbol{r}) + G^{(2)}(\boldsymbol{r}'', \boldsymbol{r})G^{(2)}(\boldsymbol{r}, \boldsymbol{r}')}. \tag{2}$$

As a direct criterion, $Q(\boldsymbol{r}, \boldsymbol{r}', \boldsymbol{r}'')$ indicates the non-Gaussianity when it deviates from 1. Galaxy surveys show that $Q \neq 1$, and confirm the non-Gaussianity of the distribution of galaxies. Moreover, Q depends on the scale and shape of the triangle (Jing & Börner 1998, 2004; Wang et al. 2004; Gaztañaga et al. 2005; Nichol et al. 2006; Gaztañaga et al. 2009; Marín 2011; McBride et al. 2011a, 2011b; Guo et al. 2016; Slepian et al. 2017), a feature also occurring in simulations (Fry et al. 1993; Barriga & Gaztañaga 2002; Gaztañaga & Scoccimarro 2005) and in the study by perturbation theory (Fry 1994; Bernardeau et al. 2002).

In this paper, as a continuation of a series of study (Zhang 2007; Zhang & Miao 2009; Zhang & Chen 2015; Zhang et al. 2019), we shall derive analytically the nonlinear field equation of $G^{(3)}$ up to second order of density fluctuation beyond Gaussian approximation, give the solution $G^{(3)}$. As have been shown

(Zhang & Li 2021), the evolution effect of correlation function of galaxies is not drastic within a low redshift range ($z = 0.5 \sim 0.0$), so for simplicity we study the nonevolution case and compare with observations ($z = 0.16 \sim 0.47$) (Marín 2011) in this preliminary work, and the evolution case will be given in future.

2. Nonlinear Field Equation of 3-point Correlation Function

Within the framework of Newtonian gravity, the distribution of galaxies and clusters in a static universe can be described by the density field ψ with the equation (Zhang 2007; Zhang & Miao 2009; Zhang & Chen 2015; Zhang et al. 2019)

$$\nabla^2\psi - \frac{(\nabla\psi)^2}{\psi} + k_J^2\psi^2 + J\psi^2 = 0, \tag{3}$$

where $\psi(\boldsymbol{r}) \equiv \rho(\boldsymbol{r})/\rho_0$ is the rescaled mass density with ρ_0 being the mean mass density, and $k_J \equiv (4\pi G\rho_0/c_s^2)^{1/2}$ is the Jeans wavenumber, c_s is the sound speed, and the source J is used to handle the functional derivatives with ease. The generating functional for the correlation functions of ψ is given by

$$Z[J] = \int D\phi \exp[-\alpha \int d^3\boldsymbol{r}\mathcal{H}(\psi, J)], \tag{4}$$

where $\alpha \equiv c_s^2/4\pi Gm$ and the effective Hamiltonian is

$$\mathcal{H}(\psi, J) = \frac{1}{2}\left(\frac{\nabla\psi}{\psi}\right)^2 - k_J^2\psi - J\psi. \tag{5}$$

The connected n-point correlation function of $\delta\psi$ is

$$\begin{aligned} G^{(n)}(\boldsymbol{r}_1,\cdots,\boldsymbol{r}_n) &= \langle\delta\psi(\boldsymbol{r}_1)\cdots\delta\psi(\boldsymbol{r}_n)\rangle \\ &= \frac{1}{\alpha^n}\frac{\delta^n \log Z[J]}{\delta J(\boldsymbol{r}_1)\cdots\delta J(\boldsymbol{r}_n)}|_{J=0} \\ &= \frac{1}{\alpha^{n-1}}\frac{\delta^{n-1}\langle\psi(\boldsymbol{r}_1)\rangle}{\delta J(\boldsymbol{r}_2)\cdots\delta J(\boldsymbol{r}_n)}|_{J=0}, \end{aligned} \tag{6}$$

where $\delta\psi(\boldsymbol{r}) = \psi(\boldsymbol{r}) - \langle\psi(\boldsymbol{r})\rangle$ is the fluctuation field around the expectation value $\langle\psi(\boldsymbol{r})\rangle$. (See Goldenfeld 1992; Zhang 2007; Zhang & Miao 2009; Zhang & Chen 2015; Zhang et al. 2019). To derive the field equation of the 3-point correlation function $G^{(3)}(\boldsymbol{r}, \boldsymbol{r}', \boldsymbol{r}'')$, we take the ensemble average of Equation (3) in the presence of J, and take the functional derivative of this equation twice with respect to the source J, and set $J = 0$. In calculation, the second term in Equation (3) is approximated by

$$\left\langle\frac{(\nabla\psi)^2}{\psi}\right\rangle = \frac{(\nabla\langle\psi\rangle)^2}{\langle\psi\rangle} + \frac{\langle(\nabla\delta\psi)^2\rangle}{\langle\psi\rangle} - \frac{\nabla\langle\psi\rangle}{\langle\psi\rangle^2} \cdot \langle\nabla(\delta\psi)^2\rangle + \frac{(\nabla\langle\psi\rangle)^2}{\langle\psi\rangle^3}\langle(\delta\psi)^2\rangle + \mathcal{O}((\delta\psi)^3), \tag{7}$$

where the second order fluctuation $(\delta\psi)^2$ is kept and higher order terms have been neglected. In this paper on the 3PCF to the second order of density perturbation, we work only up to the order $(\delta\psi)^2$, which is consistent with our previous works on the 2PCF to second order perturbation (Zhang & Miao 2009; Zhang & Chen 2015; Zhang et al. 2019). The higher order $(\delta\psi)^3$ terms in the expansion (7) are the third order of perturbation, and will be the subject of future study. By lengthy and straightforward calculations, using the definition (6), we obtain the field equation of $G^{(3)}(\boldsymbol{r}, \boldsymbol{r}', \boldsymbol{r}'')$ up to the second order of density fluctuation as the following

$$\begin{aligned}
&\nabla^2 G^{(3)}(\boldsymbol{r}, \boldsymbol{r}', \boldsymbol{r}'') + \frac{2}{\psi_0^2}\nabla G^{(2)}(0)\cdot\nabla G^{(3)}(\boldsymbol{r}, \boldsymbol{r}', \boldsymbol{r}'') \\
&+ \left(2k_J^2\psi_0 + \frac{1}{2\psi_0^2}\nabla^2 G^{(2)}(0)\right)G^{(3)}(\boldsymbol{r}, \boldsymbol{r}', \boldsymbol{r}'') \\
&- \frac{2}{\psi_0}\left(\frac{2}{\psi_0^2}G^{(2)}(0) + 1\right)\nabla G^{(2)}(\boldsymbol{r}, \boldsymbol{r}')\cdot\nabla G^{(2)}(\boldsymbol{r}, \boldsymbol{r}'') \\
&+ \left(2k_J^2 - \frac{1}{\psi_0^3}\nabla^2 G^{(2)}(0)\right)G^{(2)}(\boldsymbol{r}, \boldsymbol{r}')G^{(2)}(\boldsymbol{r}, \boldsymbol{r}'') \\
&- \frac{4}{\psi_0^3}G^{(2)}(\boldsymbol{r}, \boldsymbol{r}'')\nabla G^{(2)}(0)\cdot\nabla G^{(2)}(\boldsymbol{r}, \boldsymbol{r}') \\
&- \frac{4}{\psi_0^3}G^{(2)}(\boldsymbol{r}, \boldsymbol{r}')\nabla G^{(2)}(0)\cdot\nabla G^{(2)}(\boldsymbol{r}, \boldsymbol{r}'') \\
&+ \frac{1}{2\psi_0^2}G^{(2)}(\boldsymbol{r}, \boldsymbol{r}')\nabla^2 G^{(3)}(\boldsymbol{r}, \boldsymbol{r}, \boldsymbol{r}'') \\
&+ \frac{1}{2\psi_0^2}G^{(2)}(\boldsymbol{r}, \boldsymbol{r}'')\nabla^2 G^{(3)}(\boldsymbol{r}, \boldsymbol{r}, \boldsymbol{r}') \\
&+ \frac{2}{\psi_0^2}\nabla G^{(2)}(\boldsymbol{r}, \boldsymbol{r}')\cdot\nabla G^{(3)}(\boldsymbol{r}, \boldsymbol{r}, \boldsymbol{r}'') \\
&+ \frac{2}{\psi_0^2}\nabla G^{(3)}(\boldsymbol{r}, \boldsymbol{r}, \boldsymbol{r}')\cdot\nabla G^{(2)}(\boldsymbol{r}, \boldsymbol{r}'') \\
&- \frac{1}{2\psi_0}\nabla^2 G^{(4)}(\boldsymbol{r}, \boldsymbol{r}, \boldsymbol{r}', \boldsymbol{r}'') - k_J^2 G^{(4)}(\boldsymbol{r}, \boldsymbol{r}, \boldsymbol{r}', \boldsymbol{r}'') \\
&= \frac{1}{\alpha}\delta^{(3)}(\boldsymbol{r} - \boldsymbol{r}')G^{(3)}(\boldsymbol{r}, \boldsymbol{r}, \boldsymbol{r}'') \\
&+ \frac{1}{\alpha}G^{(3)}(\boldsymbol{r}, \boldsymbol{r}, \boldsymbol{r}')\delta^{(3)}(\boldsymbol{r} - \boldsymbol{r}'') \\
&- \frac{2\psi_0}{\alpha}\delta^{(3)}(\boldsymbol{r} - \boldsymbol{r}')G^{(2)}(\boldsymbol{r}, \boldsymbol{r}'') \\
&- \frac{2\psi_0}{\alpha}\delta^{(3)}(\boldsymbol{r} - \boldsymbol{r}'')G^{(2)}(\boldsymbol{r}, \boldsymbol{r}'),
\end{aligned} \tag{8}$$

where $G^{(2)}(0) \equiv G^{(2)}(\boldsymbol{r}, \boldsymbol{r})$ and $\psi_0 \equiv \langle\psi(\boldsymbol{r})\rangle_{J=0} = 1$, and $\nabla \equiv \nabla_{\boldsymbol{r}}$ denoting the gradient with respect to $\boldsymbol{r}$ through out the paper. When the higher order terms, such as $G^{(2)}G^{(3)}$ and $G^{(4)}$, are dropped, Equation (8) reduces to that of the Gaussian approximation. (See Equation (28) in Zhang et al. (2019).)

Yet, Equation (8) is not closed for $G^{(3)}$, as it hierarchically contains the higher order 4-point correlation function $G^{(4)}$ terms. To deal with it, we adopt the Fry–Peebles ansatz (Fry &

Peebles 1978) as the following

$$
\begin{aligned}
&G^{(4)}(\boldsymbol{r}_1, \boldsymbol{r}_2, \boldsymbol{r}_3, \boldsymbol{r}_4) = R_a[G^{(2)}(\boldsymbol{r}_1, \boldsymbol{r}_2)G^{(2)}(\boldsymbol{r}_2, \boldsymbol{r}_3)G^{(2)}(\boldsymbol{r}_3, \boldsymbol{r}_4)\\
&+ \text{sym. (12 terms)}]\\
&+ R_b[G^{(2)}(\boldsymbol{r}_1, \boldsymbol{r}_2)G^{(2)}(\boldsymbol{r}_1, \boldsymbol{r}_3)G^{(2)}(\boldsymbol{r}_1, \boldsymbol{r}_4)\\
&+ \text{sym. (4 terms)}],
\end{aligned}
\tag{9}
$$

where R_a and R_b are constants, R_a and R_b around $1 \sim 10$ roughly (Fry 1983, 1984; Meiksin et al. 1992; Szapudi et al. 1992; Peebles 1993). In absence of the theoretical knowledge of $G^{(4)}$, the Fry–Peebles ansatz has been proposed to cutoff the hierarchy. By definition $G^{(4)} \propto (\delta\psi)^4$, on the other hand, the Fry–Peebles ansatz assumes that $G^{(4)} \propto (G^{(2)})^3 \propto (\delta\psi)^6$ and therefore changes the perturbation order for the two $G^{(4)}$ terms in Equation (8). This is a price to pay when the ansatz is used to break the hierarchy. But this order change occurs at higher orders, and will not change the fundamental, linear order of the unknown function $G^{(3)}(\boldsymbol{r}, \boldsymbol{r}, \boldsymbol{r}') \propto (\delta\psi)^3$ in the equation. The error due to the ansatz is small at large distance $r \gtrsim 20$ Mpc, where $G^{(2)} \ll 1$, $G^{(3)} \ll 1$, and $G^{(4)} \ll 1$. By the ansatz (9), the $G^{(4)}$ term in Equation (8) is written as

$$
\begin{aligned}
&G^{(4)}(\boldsymbol{r}, \boldsymbol{r}, \boldsymbol{r}', \boldsymbol{r}'') = 2R_a(G^{(2)}(\boldsymbol{r}, \boldsymbol{r}') + G^{(2)}(\boldsymbol{r}, \boldsymbol{r}''))\\
&\times (G^{(2)}(0)G^{(2)}(\boldsymbol{r}', \mathrm{r}'') + G^{(2)}(\boldsymbol{r}, \boldsymbol{r}')G^{(2)}(\boldsymbol{r}, \boldsymbol{r}''))\\
&+ 2(R_a + R_b)G^{(2)}(0)G^{(2)}(\boldsymbol{r}, \boldsymbol{r}')G^{(2)}(\boldsymbol{r}, \boldsymbol{r}'')\\
&+ 2R_aG^{(2)}(\boldsymbol{r}, \boldsymbol{r}')G^{(2)}(\boldsymbol{r}, \boldsymbol{r}'')G^{(2)}(\boldsymbol{r}', \mathrm{r}'')\\
&+ R_b(G^{(2)}(\boldsymbol{r}, \boldsymbol{r}')^2 + G^{(2)}(\boldsymbol{r}, \boldsymbol{r}'')^2)G^{(2)}(\boldsymbol{r}', \mathrm{r}'').
\end{aligned}
\tag{10}
$$

Equation (8) also contains the the squeezed 3PCF,

$$
G^{(3)}(\boldsymbol{r}, \boldsymbol{r}, \boldsymbol{r}') = \frac{1}{\alpha}\frac{\delta}{\delta J(\boldsymbol{r}')}(\langle\delta\psi(\boldsymbol{r})\delta\psi(\boldsymbol{r})\rangle)|_{J=0},
$$

which is the limit $G^{(3)}(\boldsymbol{r}, \boldsymbol{r}, \boldsymbol{r}') = \lim_{\boldsymbol{r}''\to\boldsymbol{r}} G^{(3)}(\boldsymbol{r}, \boldsymbol{r}', \boldsymbol{r}'')$ (Yuan et al. 2017). When $\boldsymbol{r}'' \to \boldsymbol{r}$, the two galaxies separated by a distance $|\boldsymbol{r}'' - \boldsymbol{r}|$ will interact strongly via gravity, and $G^{(3)}(\boldsymbol{r}, \boldsymbol{r}, \boldsymbol{r}')$ will mask or distort the signals in observations and simulations. Some binning schemes are often used to avoid this difficulty (Gaztañaga et al. 2005; McBride et al. 2011a, 2011b; Slepian et al. 2017). Yuan et al. (2017) treated the squeezed 3PCF as a function of the pair-galaxy bias, independent of $|\boldsymbol{r} - \boldsymbol{r}'|$. However, observations indicate that the squeezed 3PCF Q depends on scale. Here we adopt the Groth-Peebles ansatz (Groth & Peebles 1977)

$$
G^{(3)}(\boldsymbol{r}, \boldsymbol{r}, \boldsymbol{r}') = 2QG^{(2)}(0)G^{(2)}(\boldsymbol{r}, \boldsymbol{r}') + QG^{(2)}(\boldsymbol{r}, \boldsymbol{r}')^2, \tag{11}
$$

where Q is a constant and will be treated as a new parameter in the equation of 3PCF. Even though the Groth-Peebles ansatz is correct at the Gaussian level, it changes the perturbation order. The involved terms are the squeezed terms, like $G^{(2)}(\boldsymbol{r}, \boldsymbol{r}'')G^{(3)}(\boldsymbol{r}, \boldsymbol{r}, \boldsymbol{r}')$ on the lhs of Equation (8), and the terms like $G^{(3)}(\boldsymbol{r}, \boldsymbol{r}, \boldsymbol{r}')$ in the delta source. The terms in the delta source will not affect the computing result, as they are absorbed by the boundary condition in computation. The $G^{(2)}(\boldsymbol{r}, \boldsymbol{r}'')G^{(3)}(\boldsymbol{r}, \boldsymbol{r}, \boldsymbol{r}')$ terms are of higher orders. So the use of the ansatz will not affect the linear order of the unknown function $G^{(3)}(\boldsymbol{r}, \boldsymbol{r}', \boldsymbol{r}'')$ in the equation.

Substituting (10) and (11) into Equation (8) gives the closed field equation of the 3PCF

$$
\begin{aligned}
&\nabla^2 G^{(3)}(\boldsymbol{r}, \boldsymbol{r}', \boldsymbol{r}'') + \boldsymbol{a} \cdot \nabla G^{(3)}(\boldsymbol{r}, \boldsymbol{r}', \boldsymbol{r}'')\\
&+ 2gk_J^2 G^{(3)}(\boldsymbol{r}, \boldsymbol{r}', \boldsymbol{r}'') - \mathcal{A}(\boldsymbol{r}, \boldsymbol{r}', \boldsymbol{r}'')\\
&= \frac{1}{\alpha}(2(Qb - 1) + QG^{(2)}(\boldsymbol{r}, \boldsymbol{r}''))G^{(2)}(\boldsymbol{r}, \boldsymbol{r}'')\delta^{(3)}(\boldsymbol{r} - \boldsymbol{r}')\\
&+ \frac{1}{\alpha}(2(Qb - 1) + QG^{(2)}(\boldsymbol{r}, \boldsymbol{r}'))G^{(2)}(\boldsymbol{r}, \boldsymbol{r}')\delta^{(3)}(\boldsymbol{r} - \boldsymbol{r}''),
\end{aligned}
\tag{12}
$$

where $\boldsymbol{a} \equiv \frac{2}{\psi_0^2}\nabla G^{(2)}(0)$, $b \equiv \frac{1}{\psi_0^2}G^{(2)}(0)$, $g \equiv \left(1 + \frac{1}{4\psi_0 k_J^2}c\right)$ with $c \equiv \frac{1}{\psi_0^2}\nabla^2 G^{(2)}(0)$ are three parameters, and

$$
\begin{aligned}
&\mathcal{A}(\boldsymbol{r}, \boldsymbol{r}', \boldsymbol{r}'')\\
&= 2[(R_a + R_b - 4Q + 2)b + 1]\\
&\times \nabla G^{(2)}(\boldsymbol{r}, \boldsymbol{r}') \cdot \nabla G^{(2)}(\boldsymbol{r}, \boldsymbol{r}'')\\
&- [2k_J^2 - 2k_J^2(R_a + R_b)b - (R_a + R_b - 2Q + 1)c]\\
&\times G^{(2)}(\boldsymbol{r}, \boldsymbol{r}')G^{(2)}(\boldsymbol{r}, \boldsymbol{r}'')\\
&+ (R_a + R_b - Q)b(\nabla^2 G^{(2)}(\boldsymbol{r}, \boldsymbol{r}')G^{(2)}(\boldsymbol{r}, \boldsymbol{r}'')\\
&+ G^{(2)}(\boldsymbol{r}, \boldsymbol{r}')\nabla^2 G^{(2)}(\boldsymbol{r}, \boldsymbol{r}'')\\
&+ (R_a + R_b - 3Q + 2)\boldsymbol{a} \cdot \nabla(G^{(2)}(\boldsymbol{r}, \boldsymbol{r}')G^{(2)}(\boldsymbol{r}, \boldsymbol{r}''))\\
&+ (2R_a - Q)G^{(2)}(\boldsymbol{r}, \boldsymbol{r}')G^{(2)}(\boldsymbol{r}, \boldsymbol{r}'')\\
&\times (\nabla^2 G^{(2)}(\boldsymbol{r}, \boldsymbol{r}') + \nabla^2 G^{(2)}(\boldsymbol{r}, \boldsymbol{r}''))\\
&+ (4R_a - 4Q)(G^{(2)}(\boldsymbol{r}, \boldsymbol{r}') + G^{(2)}(\boldsymbol{r}, \boldsymbol{r}''))\\
&\times \nabla G^{(2)}(\boldsymbol{r}, \boldsymbol{r}') \cdot \nabla G^{(2)}(\boldsymbol{r}, \boldsymbol{r}'')\\
&+ (2R_a - Q)(G^{(2)}(\boldsymbol{r}, \boldsymbol{r}')|\nabla G^{(2)}(\boldsymbol{r}, \boldsymbol{r}'')|^2 + G^{(2)}(\boldsymbol{r}, \boldsymbol{r}'')\\
&\times |\nabla G^{(2)}(\boldsymbol{r}, \boldsymbol{r}')|^2)\\
&+ R_aG^{(2)}(\boldsymbol{r}, \boldsymbol{r}')^2\nabla^2 G^{(2)}(\boldsymbol{r}, \boldsymbol{r}'')\\
&+ G^{(2)}(\boldsymbol{r}, \boldsymbol{r}'')^2\nabla^2 G^{(2)}(\boldsymbol{r}, \boldsymbol{r}'))\\
&+ 2R_ak_J^2(G^{(2)}(\boldsymbol{r}, \boldsymbol{r}') + G^{(2)}(\boldsymbol{r}, \boldsymbol{r}''))G^{(2)}(\boldsymbol{r}, \boldsymbol{r}')G^{(2)}(\boldsymbol{r}, \boldsymbol{r}'')\\
&+ R_aG^{(2)}(\boldsymbol{r}', \mathrm{r}'')(\boldsymbol{a} \cdot \nabla G^{(2)}(\boldsymbol{r}, \boldsymbol{r}') + \boldsymbol{a} \cdot \nabla G^{(2)}(\boldsymbol{r}, \boldsymbol{r}'')\\
&+ b\nabla^2 G^{(2)}(\boldsymbol{r}, \boldsymbol{r}') + b\nabla^2 G^{(2)}(\boldsymbol{r}, \boldsymbol{r}'') + cG^{(2)}(\boldsymbol{r}, \boldsymbol{r}')\\
&+ cG^{(2)}(\boldsymbol{r}, \boldsymbol{r}'') + \nabla^2 G^{(2)}(\boldsymbol{r}, \boldsymbol{r}')G^{(2)}(\boldsymbol{r}, \boldsymbol{r}'')\\
&+ 2\nabla G^{(2)}(\boldsymbol{r}, \boldsymbol{r}') \cdot \nabla G^{(2)}(\boldsymbol{r}, \boldsymbol{r}'')\\
&+ G^{(2)}(\boldsymbol{r}, \boldsymbol{r}')\nabla^2 G^{(2)}(\boldsymbol{r}, \boldsymbol{r}'')\\
&+ R_bG^{(2)}(\boldsymbol{r}', \mathrm{r}'')(G^{(2)}(\boldsymbol{r}, \boldsymbol{r}')\nabla^2 G^{(2)}(\boldsymbol{r}, \boldsymbol{r}')\\
&+ |\nabla G^{(2)}(\boldsymbol{r}, \boldsymbol{r}')|^2 + G^{(2)}(\boldsymbol{r}, \boldsymbol{r}'')\nabla^2 G^{(2)}(\boldsymbol{r}, \boldsymbol{r}'')\\
&+ |\nabla G^{(2)}(\boldsymbol{r}, \boldsymbol{r}'')|^2) + k_J^2(2R_abG^{(2)}(\boldsymbol{r}, \boldsymbol{r}') + 2R_abG^{(2)}(\boldsymbol{r}, \boldsymbol{r}'')\\
&+ R_bG^{(2)}(\boldsymbol{r}, \boldsymbol{r}')^2 + R_bG^{(2)}(\boldsymbol{r}, \boldsymbol{r}'')^2\\
&+ 2R_aG^{(2)}(\boldsymbol{r}, \boldsymbol{r}')G^{(2)}(\boldsymbol{r}, \boldsymbol{r}'')G^{(2)}(\boldsymbol{r}', \mathrm{r}'').
\end{aligned}
\tag{13}
$$

The function $\mathcal{A}$ depends on $G^{(2)}$. The structure of Equation (12) is similar to that in the Gaussian approximation (Zhang et al. 2019), but contains an extra convection term $\boldsymbol{a} \cdot \nabla G^{(3)}(\boldsymbol{r}, \boldsymbol{r}', \boldsymbol{r}'')$. The 2PCF $G^{(2)}(\boldsymbol{r}, \boldsymbol{r}')$ has been solved up to second order of density fluctuation (Zhang & Miao 2009; Zhang & Chen 2015; Zhang et al. 2019). In this paper, to be consistent with observation, we shall use the observed $G^{(2)}(\boldsymbol{r}, \boldsymbol{r}')$ from Marín (2011). There are eight parameters $\boldsymbol{a}$, b, c, g, Q, R_a, R_b and k_J in Equations (12) and (13), treated as being independent, which differ from those in Zhang (2007), Zhang & Miao (2009), Zhang & Chen (2015), Zhang et al. (2019) in renormalization.

3. The Solution of 3PCF Equation

In a homogeneous and isotropic universe, it is assumed that $G^{(2)}(\boldsymbol{r}, \boldsymbol{r}') = G^{(2)}(|\boldsymbol{r} - \boldsymbol{r}'|)$ and that $G^{(3)}(\boldsymbol{r}, \boldsymbol{r}', \boldsymbol{r}'')$ depends only on the configuration of a triangle with three vertexes located at $(\boldsymbol{r}, \boldsymbol{r}', \boldsymbol{r}'')$. So, $G^{(3)}(\boldsymbol{r}, \boldsymbol{r}', \boldsymbol{r}'')$ has only three independent variables, and is commonly parameterized by Marín (2011)

$$G^{(3)}(\boldsymbol{r}, \boldsymbol{r}', \boldsymbol{r}'') \equiv \zeta(s, u, \theta), \tag{14}$$

where the three variables are defined as

$$s = r_{12} \equiv r, \;\; u = \frac{r_{13}}{r_{12}}, \;\; \theta = \cos^{-1}(\hat{\boldsymbol{r}}_{12} \cdot \hat{\boldsymbol{r}}_{13}),$$

which are demonstrated in Figure 1.

Then Equation (12) is written in spherical coordinates as

$$\begin{aligned}
&\frac{1}{r^2}\frac{\partial}{\partial r}\left(r^2\frac{\partial}{\partial r}\zeta(r, u, \theta)\right) + \frac{1}{r^2\sin\theta}\frac{\partial}{\partial\theta}\left(\sin\theta\frac{\partial\zeta(r, u, \theta)}{\partial\theta}\right)\\
&+ a_r\frac{\partial\zeta(r, u, \theta)}{\partial r} + 2gk_J^2\zeta(r, u, \theta) - \mathcal{A}(r, u, \theta)\\
&= -\frac{1}{\alpha}(2b - 3Qb^2)\left(\frac{1}{|1 - u|}\frac{\delta(\theta)}{\sin\theta}\frac{\delta(r)}{2\pi r^2} + \frac{\delta(r)}{4\pi r^2}\right),
\end{aligned} \tag{15}$$

where $\xi(r) \equiv G^{(2)}(|\boldsymbol{r}|)$, a_r is the radial component of the vector parameter $\boldsymbol{a}$,

$$l \equiv |\boldsymbol{r} - \boldsymbol{r}'| = r\sqrt{1 + u^2 - 2u\cos\theta} \equiv \beta r,$$

and

$$\begin{aligned}
&\mathcal{A}(r, u, \theta) = 2[(R_a + R_b - 4Q + 2)b + 1]\beta\xi'(l)\xi'(r)\\
&+ (4R_a - 4Q)(\xi(l) + \xi(r))\beta\xi'(l)\xi'(r)\\
&- [2k_J^2 - 2k_J^2(R_a + R_b)b - (R_a + R_b - 2Q + 1)c]\xi(l)\xi(r)\\
&+ (R_a + R_b - 3Q + 2)a_r(\beta\xi'(l)\xi(r) + \xi'(r)\xi(l))\\
&+ (R_a + R_b - Q)b\left\{\left[\left(\frac{2}{r}\beta + \frac{2u}{\beta r}\cos\theta - \frac{u^2\sin^2\theta}{\beta^3 r}\right)\xi'(l)\right.\right.\\
&\left.+\left(\beta^2 + \frac{u^2}{\beta^2}\sin^2\theta\right)\xi''(l)\right]\xi(r)\\
&\left.+\left(\frac{2}{r}\xi'(r) + \xi''(r)\right)\xi(l)\right\} + (2R_a - Q)\\
&\times\left\{\xi(l)\xi(r)\left[\left(\frac{2}{r}\beta + \frac{2u}{\beta r}\cos\theta - \frac{u^2\sin^2\theta}{\beta^3 r}\right)\xi'(l)\right.\right.\\
&\left.+\left(\beta^2 + \frac{u^2}{\beta^2}\sin^2\theta\right)\xi''(l) + \frac{2}{r}\xi'(r) + \xi''(r)\right]\\
&\left.+\xi(l)\xi'(r)^2 + \xi(r)\left(\beta^2 + \frac{u^2\sin^2\theta}{\beta^2}\right)\xi'(l)^2\right\}\\
&+ R_a\left\{2\beta\xi'(l)\xi'(r)\xi(u\,r)\right.\\
&+\left(\frac{2}{r}\xi'(r) + \xi''(r)\right)(\xi(l) + \xi(u\,r))\xi(l)\\
&+\left[\left(\frac{2}{r}\beta + \frac{2u}{\beta r}\cos\theta - \frac{u^2\sin^2\theta}{\beta^3 r}\right)\xi'(l)\right.\\
&\left.\left.+\left(\beta^2 + \frac{u^2}{\beta^2}\sin^2\theta\right)\xi''(l)\right](\xi(r) + \xi(u\,r))\xi(r)\right\}\\
&+ 2R_a k_J^2(\xi(l) + \xi(r) + \xi(u\,r))\xi(l)\xi(r)\\
&+ R_a(c + 2k_J^2 b)\xi(u\,r)(\xi(l) + \xi(r))\\
&+ R_a a_r\xi(u\,r)(\beta\xi'(l) + \xi'(r)) + R_b k_J^2\xi(u\,r)(\xi(l)^2 + \xi(r)^2)\\
&+ R_a b\xi(u\,r)\left[\left(\frac{2}{r}\beta + \frac{2u}{\beta r}\cos\theta - \frac{u^2\sin^2\theta}{\beta^3 r}\right)\xi'(l)\right.\\
&\left.+\left(\beta^2 + \frac{u^2}{\beta^2}\sin^2\theta\right)\xi''(l) + \frac{2}{r}\xi'(r) + \xi''(r)\right]\\
&+ R_b\xi(u\,r)\left\{\xi(l)\left[\left(\frac{2}{r}\beta + \frac{2u}{\beta r}\cos\theta - \frac{u^2\sin^2\theta}{\beta^3 r}\right)\right.\right.\\
&\left.\times\;\xi'(l) + \left(\beta^2 + \frac{u^2}{\beta^2}\sin^2\theta\right)\xi''(l)\right]\\
&+\left(\beta^2 + \frac{u^2\sin^2\theta}{\beta^2}\right)\xi'(l)^2\\
&\left.+\xi(r)\left(\frac{2}{r}\xi'(r) + \xi''(r)\right) + \xi'(r)^2\right\}.
\end{aligned} \tag{16}$$

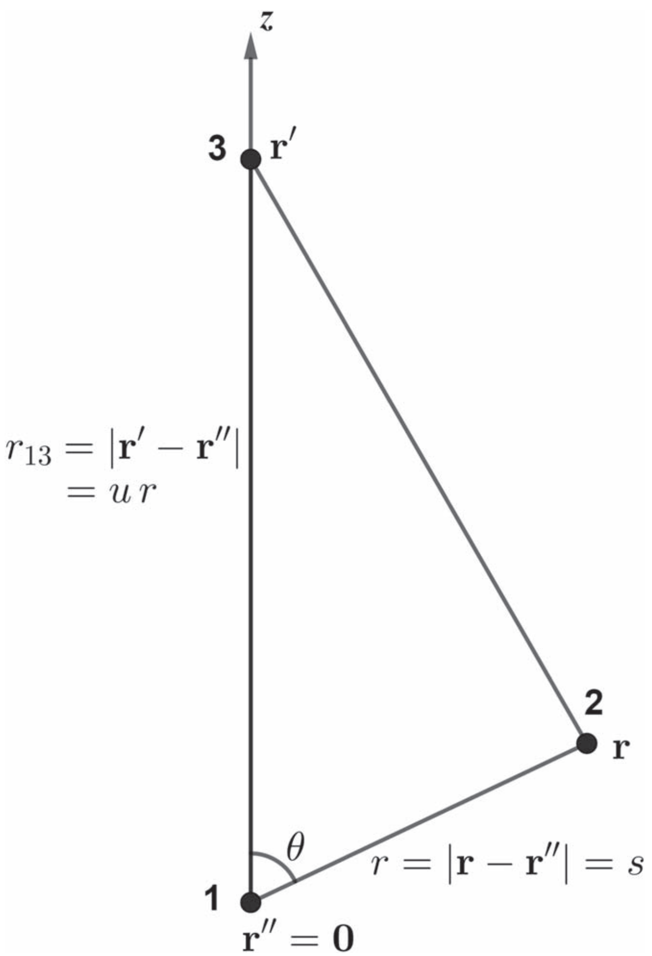

Figure 1. The configuration of the triangle of $G^{(3)}(\boldsymbol{r}, \boldsymbol{r}', \boldsymbol{r}'')$ in the spherical coordinate. Here we take the azimuth angle $\phi = 0$, $\boldsymbol{r}'' = \mathbf{0}$ as the origin, and the vector $\boldsymbol{r}' - \boldsymbol{r}''$ along with the z-axis.

Equation (15) of $\zeta(r, u, \theta)$ in spherical coordinates will be solved in actual computation. The ratio $u = 2$ is often taken in simulations and presentations of observational data, so that $\zeta(r, u, \theta)$ has only two variables. We also take this in the following.

To solve Equation (15) for ζ, we need the 2PCF $\xi(r)$. For a coherent comparison with observation, we shall use the observed $\xi(r)$ given in Figure 5 of Marín (2011). We plot Figure 2(a) to show the observed $\xi(r)$ (red with dots) from Marín (2011), and the nonlinear solution $\xi(r)$ (blue) from Zhang & Chen (2015). We also plot the function $\mathcal{A}(r, u, \theta)$ of (16) in Figure 2(b).

Besides, we also need an appropriate boundary condition on some domain. Marín (2011) has obtained the redshift-space 3PCF of luminous red galaxies of "DR7-Dim" (61,899 galaxies in the range $0.16 \leqslant z \leqslant 0.36$) from SDSS. In Figures 6 and 7 of Marín (2011), the reduced $Q(s, u, \theta)$ are given in the domain $s \in [7.0, 30.0]\ h^{-1}$Mpc, $\theta \in [0.1, 3.04]$ at five respective values $s = 7, 10, 15, 20, 30\ h^{-1}$ Mpc at a fixed $u = 2$. Specifically, we shall use the measured $Q(s, u, \theta)$ at $s = 7h^{-1}$ Mpc and $s = 30\ h^{-1}$ Mpc as a part of the boundary condition, which is fitted by

$$Q(\theta) = \begin{cases} 1.6563 + 56.8042\,\theta - 16.7962\,\theta^2 + 6.7985\cos\theta \\ \quad -6.8108\cos 2\theta - 0.4031\cos 3\theta - 54.9452\sin\theta \\ \quad -2.088\sin 2\theta + 0.7494\sin 3\theta, \qquad (s = 7.0h^{-1}\mathrm{Mpc}) \\ 86.5647 + 1040.2889\,\theta - 320.5828\,\theta^2 + 53.4609\cos\theta \\ \quad -136.5958\cos 2\theta - 2.3371\cos 3\theta - 1049.9285\sin\theta \\ \quad -14.6843\sin 2\theta + 17.0408\sin 3\theta, \qquad (s = 30.0h^{-1}\mathrm{Mpc}) \end{cases} \tag{17}$$

Also from Figures 6 and 7 of Marín (2011), we give the fitted $Q(s, u, \theta)$ at $\theta = 0.1$ and $\theta = 3.04$ as another part of the boundary condition

$$Q(s) = \begin{cases} 0.8979 + 0.039\,68\,s - 0.000\,35\,s^2, & (\theta = 0.1) \\ 1.607 - 0.08998\,s + 0.004\,731\,s^2, & (\theta = 3.04). \end{cases} \tag{18}$$

(17) and (18) lead to the boundary values of $\zeta(s, u, \theta)$ on the domain, by virtue of the relation (2). The redshift distance s is used in Marín (2011) which may differ from the real distance r due to the peculiar velocities. We shall neglect this error in our computation. To match the observational data (Marín 2011), the parameters are chosen as the following: $a_r = -1043.8\ h\mathrm{Mpc}^{-1}$, $b = -1627.3$, $c = -36.4\ h^2\mathrm{Mpc}^{-2}$, $g = -5586.6$, $R_a = 1.66$, $R_b = -0.34$, $Q = 1.1$, $k_J = 0.161\ h\mathrm{Mpc}^{-1}$.

Equation (15) is a convection–diffusion partial differential equation, and we employ the streamline diffusion method (Elman et al. 2014) to solve it numerically. We obtain the solution $\zeta(r, u, \theta)$ and the reduced $Q(r, u, \theta)$ by the relation (2).

Figure 3(a) plots the surface of $\zeta(r, u, \theta)$ as a function of (r, θ), which exhibits a shallow U-shape along θ and turns up at $\theta \gtrsim \pi/2$. This feature of solution is consistent with observations (Guo et al. 2014, 2016). $\zeta(r, u, \theta)$ decreases monotonously along r up to $30h^{-1}$ Mpc. The highest values of $\zeta(r, u, \theta)$ occur at small r and θ. For a comparison, Figure 3(b) plots the Gaussian solution $\zeta_g(r, u, \theta)$ of Equation (1), which decreases monotonously along both θ and r, having no U-shape along θ.

Figure 4 plots the surface of reduced $Q(r, u, \theta)$ as a function of (r, θ), which deviates from the Gaussianity plane $Q(r, u, \theta) = 1$, exhibits a deeper U-shape along θ, and varies along the radial r. The highest values of $Q(r, u, \theta)$ occur at large r and θ,

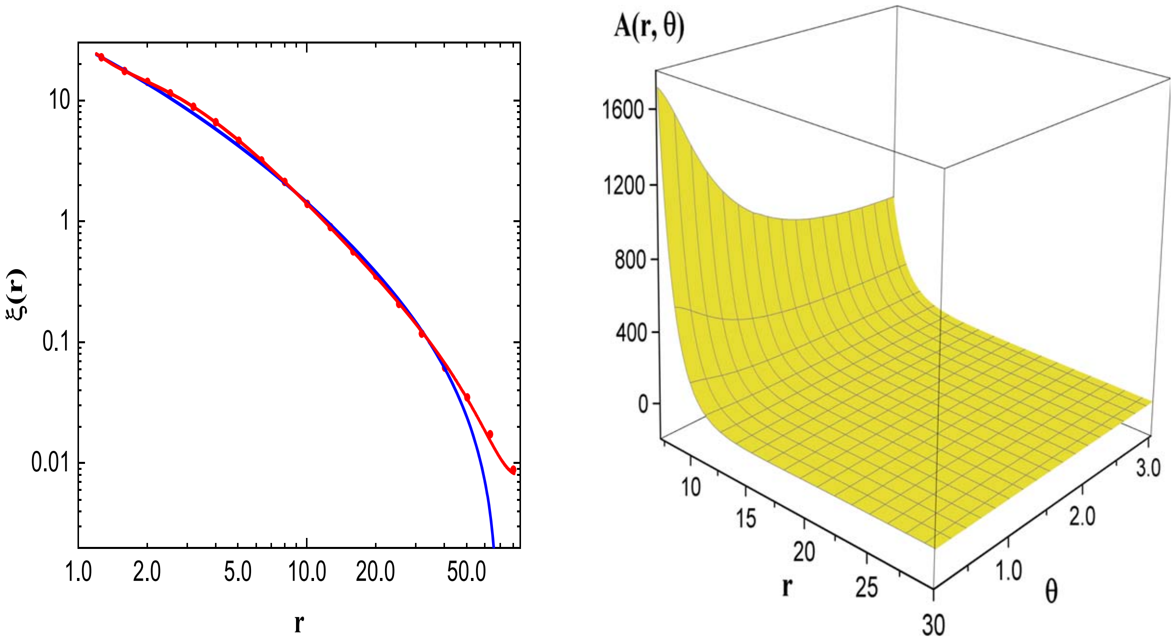

Figure 2. (a): the observed $\xi(r)$ (red with dots) from Marín (2011), the solution ξ to second order (blue) from Zhang & Chen (2015). (b): $\mathcal{A}(r, u, \theta)$ in Equation (16) at fixed $u = 2$ as function of (r, θ).

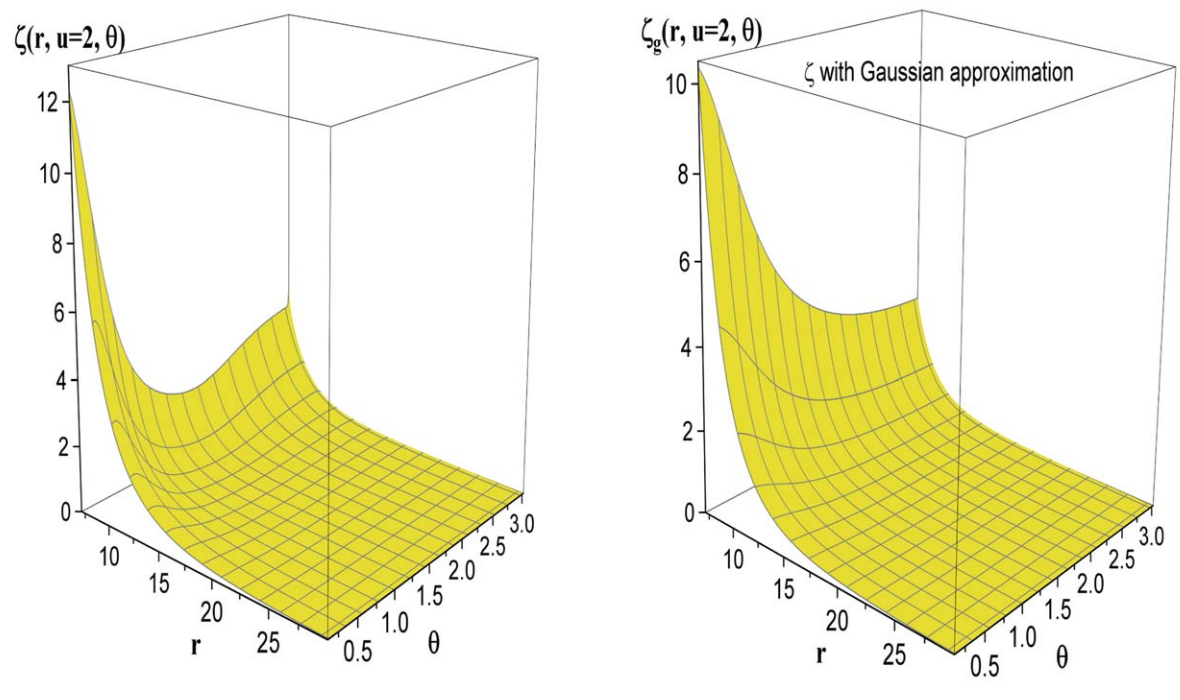

Figure 3. (a): The solution $\zeta(r, u, \theta)$ shows a shallower U-shape along θ, and decreases monotonously along r. (b): The Gaussian solution $\zeta_g(r, u, \theta)$ of Equation (1) decreases monotonously along both θ and r.

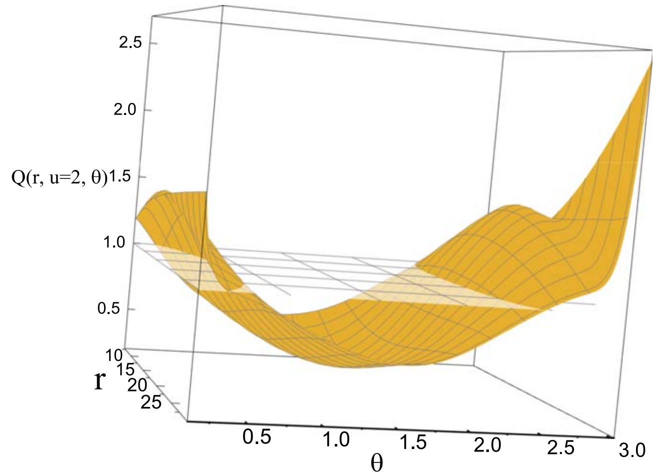

Figure 4. The surface of $Q(r, u, \theta)$ deviates from the Gaussianity plane $Q(r, u, \theta) = 1$, exhibits a deeper U-shape along θ, and varies weakly along the radial r.

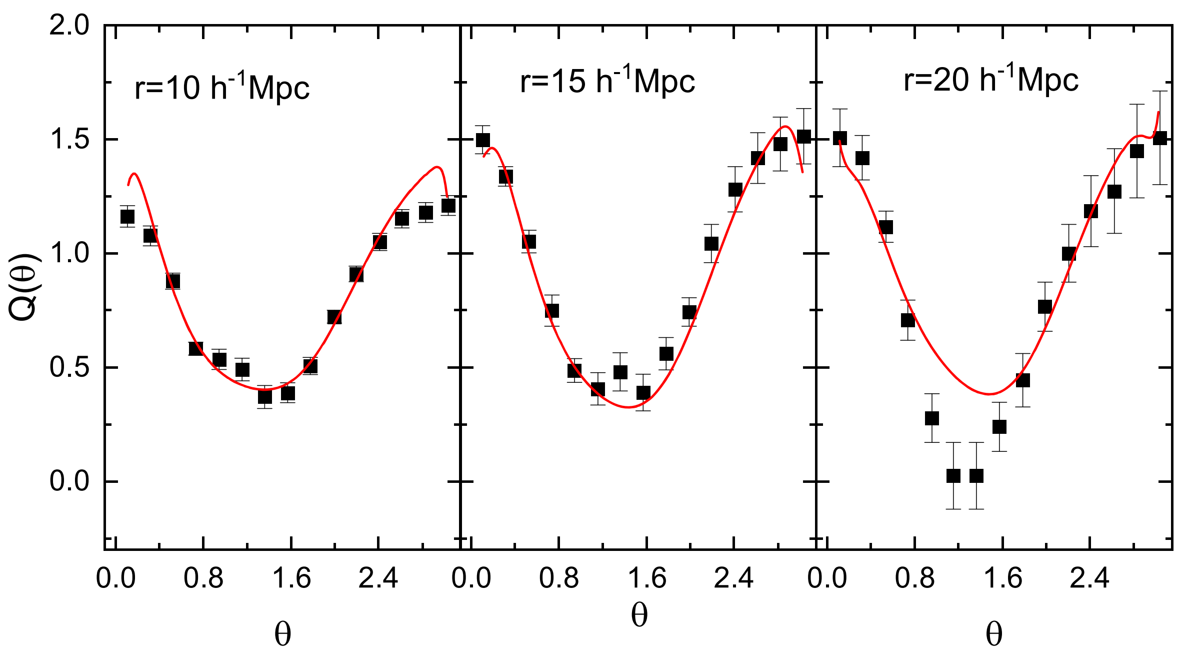

Figure 5. The solid line: $Q(r, u, \theta)$ at $u = 2$ converted from the solution $\zeta(r, u, \theta)$. The points: the SDSS observational data from Figures 6 and 7 of Marín (2011). Three plots are for $r = 10h^{-1}$Mpc, $15h^{-1}$Mpc, $20h^{-1}$Mpc, respectively. $Q(r, u, \theta)$ deviates from $Q(r, u, \theta) = 1$ of Gausianity and forms a U-shape along the elevation angle $\theta \in [0, 3]$, agreeing with the data.

just opposite to $\zeta(r, u, \theta)$. The variation along r is comparatively weaker than the variation along θ. These features are consistent with observations (Marín 2011; McBride et al. 2011a, 2011b).

To compare with observations, Figure 5 shows $Q(r, u, \theta)$ as a function of θ at respectively fixed $r = 10, 15, 20\,h^{-1}$Mpc. $Q(r, u, \theta)$ agrees well with the data of Marín (2011) available in the range $\theta = (0.1 \sim 3.0)$.

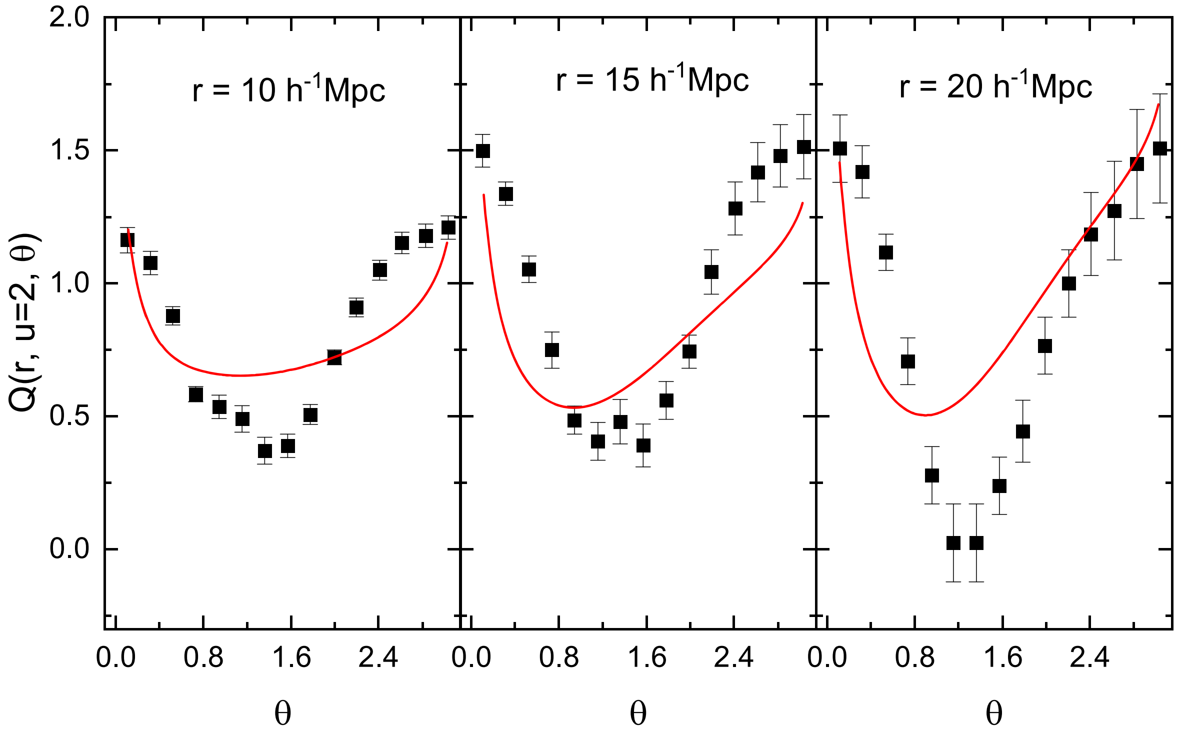

Figure 6. Similar to Figure 5. $Q(r, u, \theta)$ is plotted, using another set of parameters: $k_J = 0.12822\ h\mathrm{Mpc}^{-1}$, $a_r = 34.03\ k_J$, $b = 3.36$, $c = 1.8844\ h^2\mathrm{Mpc}^{-2}$, $R_a = -2.06$, $R_b = 6.64$, $Q = 0.7$ with $g = 1 + c/(4k_J^2)$. The fitting to the data is not as good as Figure 5.

As an example, Figure 6 plots $Q(r, u, \theta)$ with another set of parameter values, and the fitting is not as good as that in Figure 5.

4. Conclusions and Discussions

We have presented an analytical study on the 3-point correlation function of galaxies based on the field theory of density fluctuations of a Newtonian gravitating system, and have derived the nonlinear field Equation (8) of $G^{(3)}$ up to the second order density fluctuation. This work is a continuation of the previous works on the 2PCF (Zhang 2007; Zhang & Miao 2009; Zhang & Chen 2015) and on the Gaussian 3PCF (Zhang et al. 2019).

By adopting the Fry–Peebles ansatz to deal with the 4PCF, and the Groth-Peebles ansatz to deal with the squeezed 3PCF, respectively, we have made Equation (8) into the closed Equation (12) of $G^{(3)}$, equivalently Equation (15) of ζ in spherical coordinates. For coherency, we have used the observed 2PCF and the boundary condition from SDSS DR7 (Marín 2011), in solving for the 3PCF.

The solution $\zeta(r, u, \theta)$ exhibits a shallow U-shape along θ, agreeing with the observed one. Nevertheless, $\zeta(r, u, \theta)$ decreases monotonously along r, at least up to $30\,h^{-1}$ Mpc of the domain in our computation. For comparison, we also plot the Gaussian solution $\zeta_g(r, u, \theta)$, which decreases monotonously along both θ and r, having no U-shape along θ. The difference between ζ and ζ_g implies the non-Gaussianity of the distribution of galaxies.

The non-Gaussianity is directly indicated by the reduced $Q(r, u, \theta)$. The solution $Q(r, u, \theta)$ deviates from the Gaussianity plane $Q(r, u, \theta) = 1$, also exhibits a U-shape along θ, just like $\zeta(r, u, \theta)$, agreeing with the observations (Marín 2011). In fact, by its definition (2), $Q(r, u, \theta)$ shares the same θ-dependence as $\zeta(r, u, \theta)$, and its denominator consists of θ-independent $\xi(r)$. Along r, however, $Q(r, u, \theta)$ varies non-monotonically, scattering around 1, unlike $\zeta(r, u, \theta)$. Moreover, the highest values of $Q(r, u, \theta)$ occur at large r and θ, a behavior just opposite to $\zeta(r, u, \theta)$. These two features of $Q(r, u, \theta)$ are due to the behavior of $\xi(r)$ which is large at small r and suppresses $Q(r, u, \theta)$ thereby.

This preliminary study of 3PCF in this paper should be extended, and several issues need more investigation in future, such as the impact of physical parameters, exploration of parameter space in association with 2PCF, and the effect of cosmic expansion (Zhang & Li 2021).

Acknowledgments

Y. Zhang is supported by NSFC Grant Nos. 11675165, 11633001 and 11961131007 and in part by the National Key RD Program of China (2021YFC2203100).

References

Barriga, J., & Gaztañaga, E. 2002, MNRAS, 333, 443
Bernardeau, F., Colombi, S., Gaztañaga, E., & Scoccimarro, R. 2002, PhR, 367, 1
Elman, H. C., Silvester, D. J., & Wathen, A. J. 2014, Finite Elements and Fast Iterative Solvers: With Applications in Incompressible Fluid Dynamics (2nd ed.; Oxford: Oxford Univ. Press)
Fry, J. N. 1983, ApJ, 267, 483
Fry, J. N. 1984, ApJ, 279, 499
Fry, J. N. 1994, PRL, 73, 215
Fry, J. N., Mellot, A. L., & Shandarin, S. F. 1993, ApJ, 412, 504
Fry, J. N., & Peebles, P. J. E. 1978, ApJ, 221, 19
Gaztañaga, E., Cabré, A., Castander, F., et al. 2009, MNRAS, 399, 801
Gaztañaga, E., Norberg, P., Baugh, C. M., & Croton, D. J. 2005, MNRAS, 364, 620
Gaztañaga, E., & Scoccimarro, R. 2005, MNRAS, 361, 824
Goldenfeld, N. 1992, Lectures on Phase Transitions and the Renormalization Group (Frontiers in Physics vol. 85) (Oxford: Westview Press)
Groth, E. J., & Peebles, P. J. E. 1975, ApJ, 196, 1
Groth, E. J., & Peebles, P. J. E. 1977, ApJ, 217, 385
Guo, H., Li, C., Jing, Y. P., & Börner, G. 2014, ApJ, 780, 139
Guo, H., Zheng, Z., Behroozi, P. S., et al. 2016, ApJ, 813, 3
Jing, Y. P., & Börner, G. 1998, ApJ, 503, 37
Jing, Y. P., & Börner, G. 2004, ApJ, 607, 140
Marín, F. A. 2011, ApJ, 737, 97
McBride, C. K., Connolly, A. J., Gardner, J. P., et al. 2011a, ApJ, 726, 13
McBride, C. K., Connolly, A. J., Gardner, J. P., et al. 2011b, ApJ, 739, 85
Meiksin, A., Szapudi, I., & Szalay, A. S. 1992, ApJ, 394, 87
Nichol, R. C., Sheth, R. K., Suto, Y., et al. 2006, MNRAS, 368, 1507
Peebles, P. J. E. 1980, The Large-scale Structure of the Universe (Princeton, NJ: Princeton Univ. Press)
Peebles, P. J. E. 1993, Principles of Physical Cosmology (Princeton, NJ: Princeton Univ. Press)
Slepian, Z., Eisenstein, D. J., Beutler, F., et al. 2017, MNRAS, 468, 1070
Szapudi, I., Szalay, A. S., & Boschán, P. 1992, ApJ, 390, 350
Wang, Y., Yang, X., Mo, H. J., et al. 2004, MNRAS, 353, 287
Yuan, S., Eisenstein, D. J., & Garrison, L. H. 2017, MNRAS, 472, 577
Zhang, Y. 2007, A&A, 464, 811
Zhang, Y., & Chen, Q. 2015, A&A, 581, A53
Zhang, Y., Chen, Q., & We, S. G. 2019, RAA, 19, 53
Zhang, Y., & Li, B. C. 2021, PhRvD, 104, 123513
Zhang, Y., & Miao, H. X. 2009, RAA, 9, 501